ISSN 1330-3651 (Print), ISSN 1848-6339 (Online)
Received: 29 June 2025; Accepted: 20 September 2025

https://doi.org/10.17559/TV-20250629002782
Original scientific paper

Adaptive Wireless Power Transfer for Electric Vehicles: Dynamic Frequency Tuning and Intelligent Efficiency Optimization

Wei LI*, Qian WANG, Pei-chun CHEN

Abstract: Wireless Power Transfer (WPT) technology has attracted much attention because it is free from the limitations of physical cables, but its efficiency is limited by transmission distance, environmental interference and load changes. This paper presents an adaptive wireless energy transmission system with tuning and efficiency optimization of binary weighted capacitor arrays. By adjusting the resonant frequency and transmitting power in real time, combined with improved particle swarm optimization (PSO) intelligent optimization algorithm, the energy transmission efficiency and system stability can be significantly improved. The experimental results show that the power adaptive adjustment algorithm adjusts the transmit power according to SOC, and realizes fast charging, linear adjustment and trickle charging modes. Under the improved PSO strategy, the response time of the system to distance and load sudden change is less than 10 ms, the stability recovery time is less than 50 ms, and the efficiency recovery accounts for 89%, and the average efficiency of the optimized system is increased by 42.99%. When the load changes, the transmission efficiency fluctuates less than 2%, and the system has good robustness. After the introduction of metal barriers, the dynamic tuning efficiency of the system is maintained at 70.4%, and the unoptimized system efficiency is reduced to 44.6%, which indicates that the anti-interference performance of the system is good, and provides theoretical support for the design of high-efficiency wireless charging system for electric vehicles.

Keywords: binary weighting; capacitor array tuning; particle swarm optimization; wireless energy transmission

1 INTRODUCTION

With the rapid development of electric vehicle equipment, implantable medical electronics and unmanned mobile platforms, Wireless Power Transfer (WPT) technology has become a key supporting technology due to its flexibility and security. Especially in the smart home, industrial sensor networks, wearable devices and micro medical robots and other fields show irreplaceable application potential. However, traditional WPT systems face serious challenges in dynamic application scenarios: transmission efficiency fluctuates wildly with coupling coefficient, load impedance, and environmental interference. For example, the displacement or attitude change of the mobile terminal causes the relative position of the transceiver coil to shift, causing the coupling coefficient to plunge and even the resonant frequency mismatch [1]. In the scenario of multi-device coexistence, frequency band competition and cross-coupling effect will significantly reduce the stability of energy transmission [2]. In biomedical applications, differences in dielectric properties of biological tissues and the absorption effect of electromagnetic fields may lead to a surge in energy loss [3]. Existing static tuning methods (fixed frequency resonance, predefined impedance matching network) rely on preset working condition parameters, which are difficult to adapt to real-time changes in the dynamic environment, resulting in a sudden drop in system efficiency or even failure in complex electromagnetic fields, which seriously restricts the large-scale application of WPT technology [4]. Therefore, the adaptive WPT system based on dynamic tuning and efficiency optimization has become a research hotspot. Its core is to build a multi-dimensional joint state space model. By integrating multi-dimensional variables such as coil parameters (inductance, quality factor), load dynamic characteristics (impedance jump range, power demand curve), environmental interference (electromagnetic noise intensity, multipath reflection phase), etc. the closed-loop control framework of real-time perception-decision-regulation is established. In this paper, a hybrid control architecture combining deep reinforcement learning (DRL) and multi-objective particle swarm optimization (MOPSO) is proposed. DRL dynamically predicts the optimal resonant frequency and transmission power threshold through offline training and online fine-tuning strategies. Based on the Pareto frontier theory, MOPSO solves the multi-objective optimal solution set of the compensation network parameters (capacitance matrix, impedance conversion ratio) in the nanosecond time window, so as to achieve cooperative regulation in the frequency domain, time domain and energy domain. The experimental results show that the average transmission efficiency of the system can still be stable at a high level under the extreme conditions of coupling coefficient fluctuation and load impedance jump in a wide range, and the electromagnetic interference (EMI) suppression effect is better in the wide band, and the response time is better than the traditional PID control. Further, compared with the static tuning method, the efficiency of the system in dynamic scenarios is significantly improved, providing a scalable technical paradigm for highly robust wireless power supply, which can be extended to the frontier fields of UAV group collaborative charging and in-body nanorobots energy supply in the future.

The rest of this paper is as follows. Section 2 introduces the research status of dynamic tuning and efficiency optimization technology. Sections 3 and 4 describe the research methods of this subject. The experimental results of this study are given in section 5.

2 LITERATURE REVIEW

In recent years, research on improving the efficiency of wireless power transfer (WPT) has gained increasing attention, with various algorithms and methodologies contributing to significant enhancements in system performance. Sim et al. (2023) [5-7] proposed a rapid and efficient coil optimization method for WPT systems based on Bayesian optimization. This approach accounts for the complexity of ferrite materials and coil design, utilizing Bayesian optimization to achieve high-efficiency energy transfer. In a study by Xu et al. (2024) [8-10], a tracking method based on full-current mode impedance matching

was introduced to optimize WPT efficiency. This technique not only enables efficient tracking but also allows seamless switching between continuous and discontinuous conduction modes, thereby extending the detection capabilities of WPT systems. Yang et al. (2024) [11, 12] investigated the tuning of PI parameters for frequency tracking control using an improved whale optimization algorithm. Their research underscores the critical importance of effective frequency tracking in maintaining high-efficiency energy transfer. Innovations such as chaotic mapping and adaptive weighting significantly improved the algorithm's convergence and global search capabilities. Gao et al. (2023) [13-15] applied particle swarm optimization to maximize efficiency in WPT systems. The authors noted that conventional impedance matching methods, which rely on simplified circuit models, introduce certain inaccuracies. Chawla et al. (2023) [16] proposed a nearly constant power tuning network to address the relationship between output power and coupling coefficient variations in inductive wireless power transfer systems. By introducing a parallel resonant series (PRS) tuning method, their study demonstrated effective mitigation of power fluctuations caused by coil misalignment while maintaining high efficiency and achieving zero-voltage switching. Similarly, Rong et al. (2023) [17-19] focused on wireless power transfer for concrete-embedded sensors and introduced a composite tuning control technique to counteract electromagnetic disturbances caused by concrete materials. Through a combination of frequency modulation tuning and dynamic compensation tuning, the study illustrated how the natural resonant frequency can be adjusted to ensure system-wide resonance. Li et al. (2023) [20-22] proposed a dynamic tuning control method based on variable inductance, specifically addressing detuning caused by variations in resonant parameters in multi-relay WPT systems. Chen et al. (2022) [23] developed a dynamic wireless power transfer (DWPT) system that enables real-time charging of electric vehicles in motion, substantially improving transportation efficiency. Liu et al. (2022) [24, 25] explored a strongly coupled coaxial three-coil WPT system, demonstrating that adjusting the relative position of relay coils significantly enhances both transmission distance and efficiency. Research by L. Mason, T. Drwiega [14], and James Yan [26-28] (2007) focused on traffic performance management in converged networks, employing game-theoretic models between internet service providers (ISPs) and between ISPs and customers, providing a theoretical foundation for adaptive wireless power transfer technologies. In contrast to traditional technology-driven approaches, the work of Mason et al. [29, 30] highlights the importance of integrating economics and network science. Through game-theoretic modeling, they revealed the complexities of traffic management in diverse user demand and network environments.

Despite notable technological advancements, three major research gaps remain: First, algorithm validation predominantly relies on simulations or idealized experimental conditions, lacking empirical studies in complex real-world scenarios such as multipath interference and non-ideal electromagnetic environments which raises concerns about algorithmic robustness and adaptability. Second, the applicability of dynamic tuning technologies in complex environments, including interference from metallic objects and resonant mismatches under dynamic load variations, has not been systematically investigated. Third, the synergistic relationship between algorithms and tuning techniques remains underexplored. Most theoretical frameworks focus on a single technical dimension, lacking systematic cross-technology analysis - for instance, how optimization algorithms influence the real-time response of tuning networks, or how tuning strategies affect algorithmic convergence. Moreover, few studies explicitly quantify the trade-off between algorithmic complexity and system real-time performance, limiting practical deployment.

To address these gaps, this paper proposes an adaptive WPT system based on a tunable capacitor array for dynamic tuning and efficiency optimization. A tripartite research framework integrating theory, simulation, and empirical validation is established. By combining control theory and game theory, a multi-agent interactive dynamic tuning model is developed to quantify the trade-off between algorithmic complexity and real-time performance. A multi-physics digital twin platform is also constructed to simulate complex scenarios such as metallic interference and load fluctuations, thereby validating algorithm performance under non-ideal conditions.

3 PROPOSED SYSTEM DESIGN AND METHODOLOGY

3.1 Adaptive WPT System Architecture

The adaptive WPT system consists of the following modules, as shown in Fig. 1. The transmitting end is composed of a high-frequency inverter, a dynamic tuning unit and a control unit. The receiving end is composed of a resonant coil, a rectifying circuit, a DC-DC circuit, a load and a feedback module (including a sensor and a Bluetooth communication unit). The central controller of transmitter and receiver uses FPGA, integrates dynamic tuning algorithm and efficiency optimization model. Load impedance and environmental parameters are monitored by sensors at the receiving end and fed back to the transmitting end. The transmitter adopts PID control algorithm to adjust the inverter frequency, so that the system is always in a resonant state.

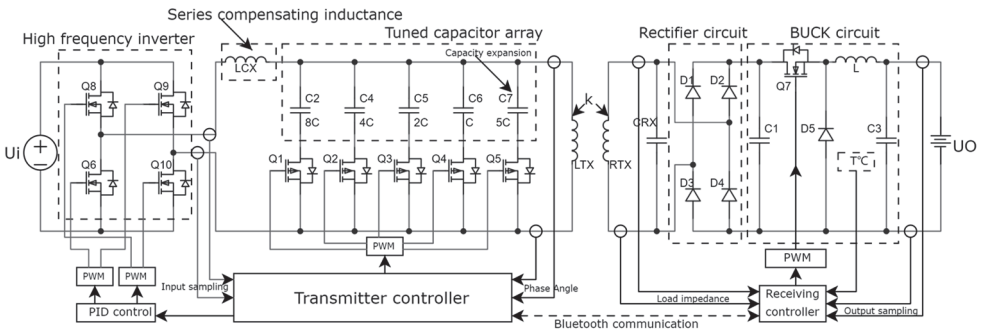

Figure 1 Block diagram of system composition

3.2 Dynamic Tuning Mechanisms

3.2.1 Real-time Resonant Frequency Matching Algorithm

The real-time matching process of resonant frequency is usually realized by closed-loop control system: Firstly, the sensor is used to monitor the voltage and current phase difference of the circuit in real time to obtain the current working state. Secondly, the monitoring data (phase deviation, minimum reflected power position) is compared with the preset resonance conditions to determine whether there is a mismatch. If there is a deviation, the PI control algorithm, linear sweep frequency and comparator are used to dynamically adjust the excitation source frequency, so that the system always tracks the natural resonance frequency. In Figure 1, the mathematical modeling of real-time resonance frequency matching is shown as follows:

$$f_{\text{res}} = \frac{1}{2\pi\sqrt{L_{\text{eq}}C_{\text{eq}}}} \tag{1}$$

where, L_{eq} and C_{eq} are equivalent inductance and capacitance respectively. f_{res} is the resonant frequency.

3.2.2 Adaptive Power Regulation Strategy

The power adaptive adjustment algorithm dynamically optimizes the output through closed-loop feedback. The realization process is to collect the load current, voltage and temperature parameters in real time, combined with the preset efficiency model, and use the fusion algorithm to calculate the optimal power point online. The transmission power is dynamically adjusted by PWM modulation and FPGA control, and the balance between efficiency and loss is realized. According to the charging state of the receiving battery, the system dynamically adjusts the transmitting power to avoid energy waste. The power adaptive adjustment algorithm of this system is designed as follows:

(1) The receiving end regularly detects the battery *SOC* and sends it to the transmitting end.

(2) The transmitting end calculates the power to be adjusted according to the current *SOC*, target *SOC*, and current transmitting power.

(3) PID control is used to adjust the power according to the error (target *SOC* - current *SOC*), at the same time, fuzzy logic control is used to deal with nonlinear relations.

(4) Ensure that the power adjustment is within the safe range, not exceeding the maximum power of the transmitter, not less than the minimum power.

The specific algorithm logic is as follows:

The first step, Feedback acquisition. The receiving end periodically detects SOC_{current} and feeds back to the transmitting end via the communication link (BLE).

The second step, Error calculation. The charging error e is calculated by the following formula:

$$e = SOC_{\text{target}} - SOC_{\text{current}} \tag{2}$$

where, SOC_{current} indicates the current battery charging state (0% to 100%). SOC_{target} is the target charging state (100%);

The third step, Power adjustment

Phase 1 (Fast charging): When $e > 20\%$, charge at the maximum power $P_{\max}$.

Phase 2 (proportional adjustment): When $5\% \le e \le 20\%$, adjust the power proportionally. The proportional adjustment formula is as follows:

$$P = \min(K_{\text{p}} \cdot e, P_{\text{req\_max}}, P_{\max}) \tag{3}$$

where, K_{p} is the proportional coefficient; $P_{\text{req\_max}}$ is the maximum acceptable power at the receiving end, which is determined by the battery circuit. $P_{\max}$ is the maximum transmitting power at the transmitting end; $P_{\min}$ is the minimum transmitting power at the transmitting end;

Phase 3 (trickle charging): When $e < 5\%$, $P_{\min}$ is used to maintain charging to avoid overcharging.

Phase 4: When $SOC_{\text{current}} \ge SOC_{\text{target}} - H_{\text{ysteresis}}$, the transmit power is disabled. $H_{\text{ysteresis}}$ indicates the hysteresis interval to avoid threshold shock.

In the above algorithm, in order to improve the reliability of the system, constraints are set. The constraints are composed of power dynamic constraints and battery *SOC* constraints, which are as follows:

Power dynamic constraints:

$$P_{\min} \le P \le \min(P_{\max}, P_{\text{req\_max}}) \tag{4}$$

Battery *SOC* constraints:

$$\begin{cases} P \ge K_{\text{fast}} \cdot e, e > 20\%; \\ P \le K_{\text{fast}} \cdot T_{\max}^{-1}; \end{cases} \tag{5}$$

Among them, the second term is the temperature protection constraints.

3.2.3 Efficiency Optimization Model

The nonlinear relationship between the efficiency of transmitter and receiver with power is considered. For example, at certain power points, the conversion efficiency may be higher, and simple proportional adjustment is not optimal. Therefore, adaptive regulation requires efficiency optimization.

(1) Construction of efficiency optimization model

The optimization model is implemented using the efficiency-power curve [31]. It is completed by constructing the objective function. In the design, the objective function is defined as maximizing the relationship between transmission efficiency and power. It can be divided into transmitter efficiency-power relationship, receiver efficiency-power relationship and total efficiency-power relationship.

The efficiency-power relationship at the transmitting end is calculated as follows:

$$\eta_{Tx}(P) = \begin{cases} a_1 \cdot e^{-b_1 P} + C_1 \\ 0 < P \le P_{\max} \end{cases} \tag{6}$$

The efficiency-power relationship at the receiving end is calculated as follows:

$$\eta_{Rx}(P)=\begin{cases} a_2\cdot\dfrac{P}{P+b_2}+C_2 \\ P_{\min}\le P\le P_{\text{req\_max}} \end{cases} \tag{7}$$

The total efficiency-power relationship is calculated as follows:

$$\eta_{\text{total}}(P)=\eta_{Tx}(P)\cdot\eta_{Rx}(P) \tag{8}$$

In the design, the efficiency values under different power were measured by experiment, and the coefficients a_1, b_1, c_1, a_2, b_2, c_2 were fitted by nonlinear regression.

In Eq. (8), the model of maximizing effective transmission energy is adopted to define the optimization results, and the expression is as follows:

$$P_{\max}=\eta_{\text{total}}(P)\cdot P\cdot\Delta t-\lambda\cdot(P-P_{\text{prev}})^2 \tag{9}$$

In Eq. (9), the first term on the right is the process of maximizing transmission energy efficiency; The second term is the power change smoothing term to avoid sharp fluctuations in power, resulting in low efficiency. Set the following constraints in the implementation:

$$\begin{cases} e=SOC_{\text{target}}-SOC_{\text{current}}; \\ P_{\min}\le P\le\min(P_{\max},P_{\text{req\_max}}); \\ \eta_{\text{total}}(P)\ge\eta_{\text{threshold}}; \\ \mathrm{d}T/\mathrm{d}t\le K_{\text{temp}}\cdot P^2; \end{cases} \tag{10}$$

Among them, the first item is the constraints of the load battery; The second term is the transmission power constraints; The third is the constraint condition of conversion efficiency; The fourth item is the constraint condition of temperature change rate, and K_{temp} is the compensation coefficient of temperature constraint, which can be measured experimentally.

4 ENHANCED PARTICLE SWARM OPTIMIZATION (PSO) ALGORITHM FOR EFFICIENCY IMPROVEMENT

4.1 Overview of the Improved PSO Algorithm

The optimization algorithm framework is shown in Fig. 2.

In the optimization model, the algorithm enhancement design is carried out according to the nonlinear and multi-constraint characteristics of wireless energy transmission system. The system is optimized from the resonant frequency and power distribution to achieve the dynamic adaptability and efficiency of the system in the case of multiple objectives, so as to ensure that the optimal solution is quickly found in the complex environment and improves the energy transmission efficiency. In the design, based on particle swarm optimization [32-34], the inertial weight adaptive mechanism is introduced to balance the global search and local convergence capabilities, so as to optimize the resonant frequency and power distribution.

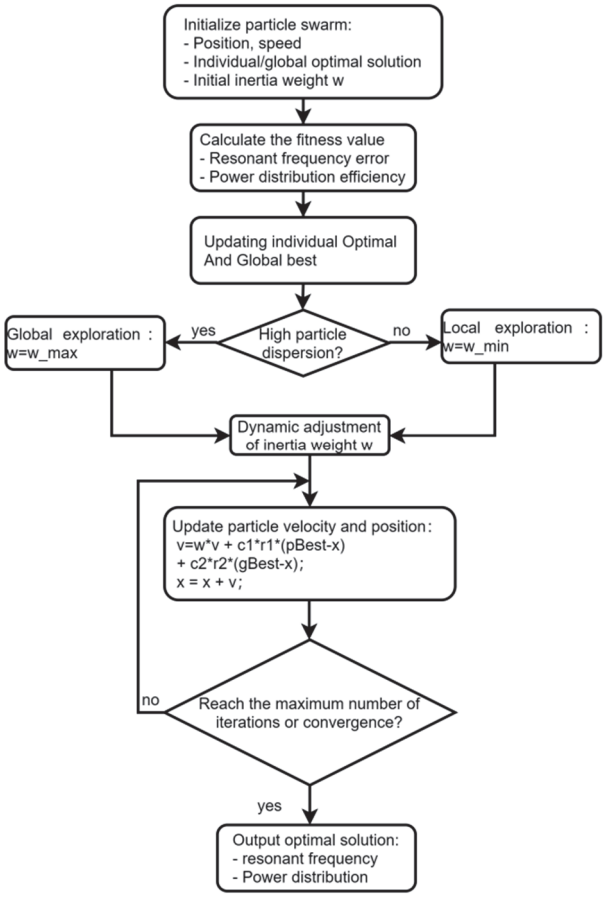

Figure 2 POS optimization algorithm framework

4.2 Objective Function Formulation

The design method is as follows:

First step, establish the objective function of PSO algorithm

The objective function is expressed by maximizing comprehensive efficiency, and the formula is as follows:

$$\begin{aligned} &\text{Maximize}\,\eta_{\text{total}}=\eta_{\text{coupling}}(f)\times\eta_{\text{power}}(\alpha) \\ &-\lambda\cdot\text{Im}\,balance(\alpha) \end{aligned} \tag{11}$$

where, f is the resonant frequency, α assigns weight to the power in the multiple-emitter scenario, and the value range is [0-1]. The total conversion efficiency of $\eta_{\text{power}}(\alpha)$ when multiple transmitters work together can be obtained by Eq. (8). $\eta_{\text{coupling}}(f)$ is the coupling efficiency. The coupling efficiency is calculated as follows:

$$\eta_{\text{coupling}}=\frac{|S_{21}a_1+S_{22}a_2|^2}{|a_1|^2-|S_{11}a_1+S_{12}a_2|^2}=\frac{|S_{21}|^2}{1-|S_{11}|^2} \tag{12}$$

where S is the reflection coefficient.

In Eq. (11), Imbalance (α) is a penalty term of equilibrium, which prevents overload of a single emitter. The calculation formula is as follows:

$$\text{Im}\,balance(\alpha)=\sum(\alpha_i-\alpha)^2 \tag{13}$$

At the same time, in the equilibrium penalty term, certain constraints are needed to prevent convergence too

fast and overstepping the boundary. The constraints are as follows:

$$\begin{cases} f_{\min} \le f \le f_{\max}; \\ \sum \alpha_i = 1; \\ T_j \le T_{\max}; \\ P_k \le P_k^{\max}; \end{cases} \tag{14}$$

where, $T_{\max}$ is the maximum temperature of each node; $P_k^{\max}$ is the maximum value of a single transmit power.

4.3 Dynamic Adjustment of PSO Parameters

Dynamic adjustment strategy of inertia weight. The inertia weight adaptive mechanism is introduced in PSO algorithm. The algorithm should enhance the global search in the initial stage, and improve the local search ability in the later stage. This task is completed by configuring dynamic inertia weights. The configuration formula is as follows:

$$\omega(t) = \omega_{\max} - (\omega_{\max} - \omega_{\min}) \cdot (\frac{t}{t_{\max}})^2 + \\ +\sigma \cdot rand() \tag{15}$$

The parameters are set as follows:

At the initial stage, $w_{\max} = 0.9$ is set to enhance the global search capability of the algorithm. In the later stage, set $w_{\min}$ to 0.4 to improve local convergence. The random disturbance term σ is set to 0.1 to avoid premature convergence and enhance the ability to jump out of the local optimal.

The third step, Learning factor selection

The algorithm also needs to select appropriate adaptive learning factors. There are two adaptive learning factors, which are used to dynamically adjust the weight of individual experience and social experience to accelerate convergence. Among them, g_1 focuses on individual cognition in the early stage and g_2 focuses on social experience in the late stage, as follows:

$$\begin{cases} g_1 = c_{1,\text{initial}} - \Delta c \times \frac{t}{t_{\max}}; \\ g_2 = c_{2,\text{initial}} + \Delta c \times \frac{t}{t_{\max}}; \end{cases} \tag{16}$$

In the design, $C_{1,\text{initial}}$ value 2.5, $C_{2,\text{initial}}$ value 0.5, Δc value 2, accelerate convergence.

4.4 Elite Preservation and Mutation Strategies

Construct elite retention and variation mechanism. The goal of the elite retention and mutation mechanism is to keep the algorithm diverse. Maintain population diversity while avoiding premature convergence.

The first is to retain the top 5% of fitness particles (elite particles) in each generation and do not participate in regular speed updates.

Secondly, Gaussian variation is performed on the stationary particle (which has not been improved for many generations), and the formula is as follows:

$$\begin{cases} x_{\text{new}} = x_{\text{old}} + N(0, \sigma^2); \\ \sigma = 0.1 \cdot (x_{\max} - x_{\min}); \end{cases} \tag{17}$$

The fifth step, Construction of constraints

In Eq. (11), Eq. (15), Eq. (16), Eq. (17), in order to prevent the algorithm from overstepping the bounds, the algorithm constraints are constructed. The constraint conditions include power distribution constraint, frequency boundary constraint and penalty function as follows:

$$\begin{cases} \alpha_i^{\text{new}} = \frac{\alpha_i^{\text{old}}}{\sum \alpha_j^{\text{old}}}; \\ f_{\text{new}} = \min(\max(f_{\text{old}}, f_{\min}), f_{\max}); \\ Fitness_{\text{penalized}} = Fitness - \varsigma \cdot e^{\xi \cdot ViolationDegree}; \end{cases} \tag{18}$$

Among them, the first term is power distribution constraint; the second term is frequency boundary constraint; the third term is the penalty function. ζ is the punishment coefficient and ξ punishment intensity factor. α_i^{new} is the normalized projection and f_{new} is the boundary constraint frequency. $Fitness_{\text{penalized}}$ is a penalty function that forces particles to move toward the feasible region.

5 IMPLEMENTATION OF DYNAMIC TUNING AND CONTROL CIRCUITS

5.1 Binary-Weighted Capacitor Array Design

The dynamic tuning circuit realizes dynamic resonance management through real-time detection-algorithmic decision-fast closed-loop control. The circuit design mainly includes two parts: one is the tuning circuit, the second is matching network design. The tuning circuit design is realized by variable capacitor array, and the capacitor value is switched by MOSFET switch to achieve fine tuning of resonant frequency. The resonant Eq. (1) is used to derive the corresponding capacitance range. The formula is as follows:

$$C_{\min} = \frac{1}{(2\pi f_{\max})^2 L} \tag{19}$$

$$C_{\max} = \frac{1}{(2\pi f_{\min})^2 L} \tag{20}$$

The design tuning frequency range is 10 MHz to 30 MHz. The resonant inductance L is 100 nH, and the calculation is as follows: $C_{\min} = 2.8$ pF, $C_{\max} = 25.3$ pF.

The design of capacitor array adopts binary weighted structure. Use N-bit capacitors, each with a capacitance value of C, $2C$, $4C$, ..., $2^{n-1}C$. Total capacitance: $C_{\text{total}} = C \times (2^n - 1)$, covering $C_{\min}$ to $C_{\max}$.

In the design of the dynamic tuning circuit, a 4-bit binary array is used to provide 16 combinations, and the

step is 1 pF. The capacitance values are selected as 1 pF, 2 pF, 4 pF, 8 pF, so as to cover 1 pF to 15 pF, and then the parallel fixed capacitance 5 pF extends to a maximum of 35 pF, so as to cover 2.8 pF to 25.3 pF. The circuit topology is shown in Fig. 3.

Due to the parasitic capacitance of MOSFET, in order to improve the adjustment accuracy, parasitic parameter compensation is carried out in the design. That is, when calculating the total capacitance, C_{oss} is introduced for each disconnected MOSFET, then the total capacitance is corrected to:

$$C_{\text{total}} = \sum_{\text{on}} C_i + \sum_{\text{off}} C_{\text{oss}} \tag{21}$$

C_{oss} values for MOSFET are available in the device manual.

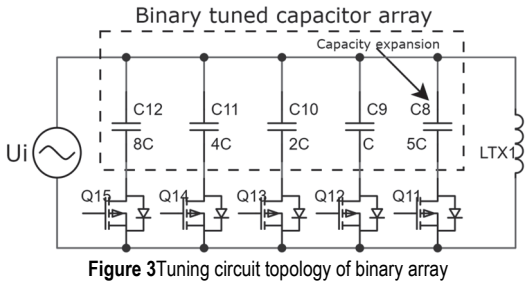

Figure 3 Tuning circuit topology of binary array

5.2 Impedance Matching Network Design

The *L*-type matching network is used to compensate the variation of coupling coefficient between coils.

(1) Mutual inductance model. The change of coupling coefficient k between coils leads to the change of mutual inductance *M*. *M* is calculated as follows:

$$M = k\sqrt{L_1 \times L_2} \tag{22}$$

The equivalent impedance reflected from the secondary coil impedance to the primary side is the reflected impedance, which is calculated as follows:

$$Z_{\text{ref}} = \frac{(\omega M)^2}{Z_{\text{load}} + j\omega L_2 + R_2} \tag{23}$$

where Z_{load} is the load impedance and R_2 is the secondary coil resistance.

(2) *L*-type matching network design

According to the relationship between source impedance Z_S and reflected impedance $Z_{ref,}$ the *L*-type matching network structure is designed as series *L* + parallel *C* structure, as shown in Fig. 4.

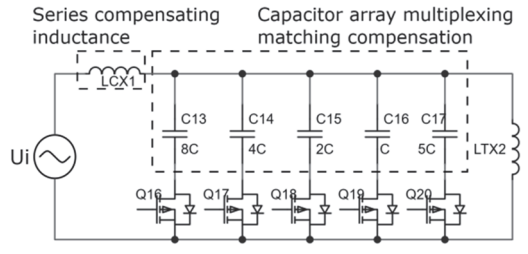

Figure 4 L-type matching network structure

Inductance and capacitance are calculated as follows:

$$LC_X = \frac{\sqrt{Z_S(Z_{\text{ref}} - Z_S)}}{\omega} \tag{24}$$

$$C_{CX} = \frac{1}{\omega\sqrt{Z_S(Z_{\text{ref}} - Z_S)}} \tag{25}$$

(3) Dynamic compensation

In the circuit design, the MOSFET switching capacitor array in the dynamic tuning circuit is reused and the shunt capacitor value *C* is adjusted. The Z_{ref} variation range is then calculated by dividing the maximum value of *k* by the minimum value, thus determining C_{min} and C_{max}. Calculate *k* value in real time by FPGA and switch array capacitor combination.

5.3 Feedback Control Framework

There are three main factors affecting system stability in feedback control, which are time temperature, impedance and receiving power. An increase in temperature (*T*) leads to an increase in the internal resistance of the device, which further affects the power and impedance. At the same time, impedance variation (Z_L) directly affects the power transmission efficiency. In the design, the feedback control adopts the multi-parameter feedback mode, that is, the receiving end transmits the load impedance, received power and temperature data to the controller in real time, and the controller receives these data information through the improved PSO algorithm to optimize the resonant frequency and power distribution of the system. The state equation of the control strategy is shown as follows:

$$\begin{cases} \dfrac{\mathrm{d}P}{\mathrm{d}t} = f(P, Z_{\text{L}}, T); \\ \dfrac{\mathrm{d}Z_{\text{L}}}{\mathrm{d}t} = g(P, T); \\ \dfrac{\mathrm{d}T}{\mathrm{d}t} = h(P, Z_{\text{L}}); \end{cases} \tag{26}$$

Among them, the influence relationship of temperature is as follows:

$$R(T) = R_0(1 + \alpha\Delta T) \tag{27}$$

6 EXPERIMENTAL VALIDATION AND PERFORMANCE ANALYSIS

6.1 Experimental Setup and Test Conditions

The transmitting power is 120 W, the operating frequency is 16 MHz, and the dynamic tuning coil diameter is 20 cm. The resonant coil at the receiving end has a diameter of 15 cm, and the load is of two types: battery and variable resistance. The *SOC* is set to less than 30% before the battery starts charging, and the variable resistance ranges from 0 to 50 Ω. The test scenarios are divided into two categories: fixed-distance test and dynamic distance

test. The distance between the transmitting coil and the receiving coil is maintained at a fixed distance of 20 cm. The first test is to connect the battery at the receiving end for charging. The single lithium battery is with a cut-off voltage of 4.2 V and a maximum charging current of 2 A. The second is to use variable resistance as a load, resistance from 10 Ω to 30 Ω step change. The third is the dynamic distance test, the distance change range of 10 cm to 40 cm, at this time the receiving end of the load using a constant load, resistance value of 10 Ω. The completed experimental platform is shown in Fig. 5.

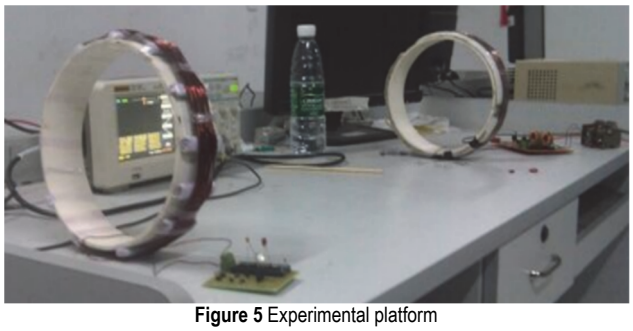

Figure 5 Experimental platform

6.2 Performance of Adaptive Power Regulation

At a fixed distance, the battery is discharged to 30% *SOC* and then connected to the system. The *SOC* curve of the battery varies with the transmitted power, as shown in Fig. 6.

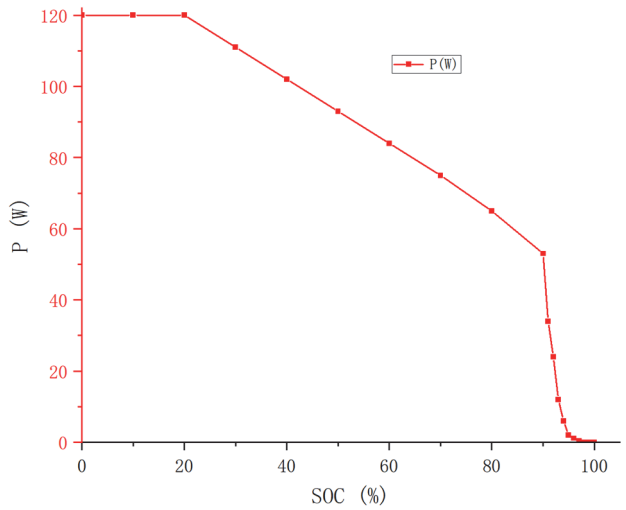

Figure 6 *SOC* transformation curve of battery charging

In Fig. 6, when the *SOC* is less than 30%, the transmitted power is full power output (120W) to achieve fast charging. When *SOC* ranges from 30% to 75%, the proportional adjustment of transmit power decreases, showing linear characteristics. When *SOC* range is 75%-95%, the transmitted power enters trickle charging mode. When the *SOC* is 98%, the transmitting power becomes 0 and the charging stops. The whole process is in complete agreement with the design algorithm.

6.3 Efficiency Optimization under Various Conditions

The test scenario is divided into three types. The first set the *SOC* of the battery at 30% and the temperature at room temperature (25 ℃), and measured the maximum charging speed (maximum charging current). Under the conditions of 0.5 C, 1.0 C and 1.5 C, *SOC* changes from 30% to 80% were recorded respectively. Record the terminal voltage change process of the battery. The measurement results are shown in Fig. 7 below.

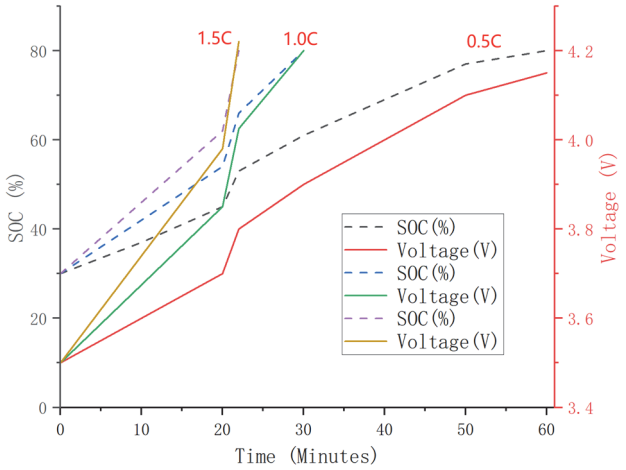

Figure 7 Measurement of maximum charging speed

At 25 ℃ and *SOC* 30%, the maximum safe charging speed of the battery is 1.0 C (30 minutes to 80%).

In the second group, *SOC* was set at 85%, and the temperature ranged from room temperature 25 ℃ to high temperature 85 ℃. The relationship between efficiency and temperature was measured, and the measurement results are shown in Fig. 8 below.

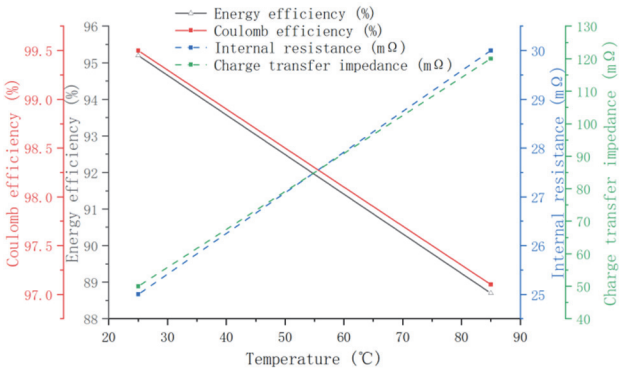

Figure 8 Relationship between efficiency and temperature

In Fig. 8, when the temperature rises from 25 ℃ to 85 ℃, the energy efficiency decreases by 6.5% and the charge transfer impedance increases by 140%.

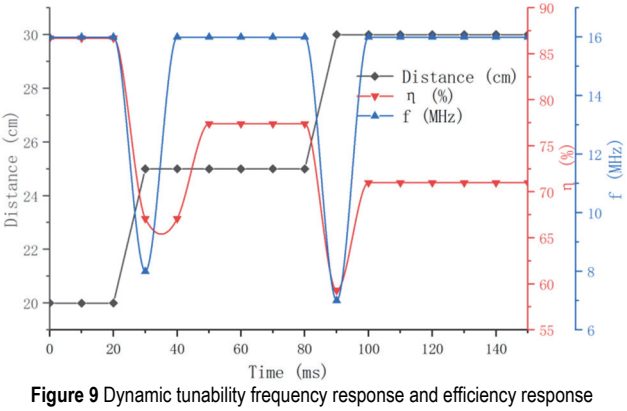

Figure 9 Dynamic tunability frequency response and efficiency response

The third group is to change the distance between the transmitting coil and the receiving coil (20 cm to 30cm), the resonant frequency is 16 MHz, and the dynamic tuning frequency response and efficiency response are measured. The measurement results are shown in Fig. 9.

In Fig. 9, the frequency response time is less than 10 ms, and the recovery time is less than 20 ms. The efficiency response time is about 12 ms, the recovery time is less than 30 ms, and the overall efficiency decreases by 15.7%.

6.4 Dynamic Tuning Performance Evaluation

At a fixed distance, the load changes (10ω changes to 20 Ω), the resonant frequency of the measurement system changes, and the conversion efficiency changes. The test results are shown in Fig.10.

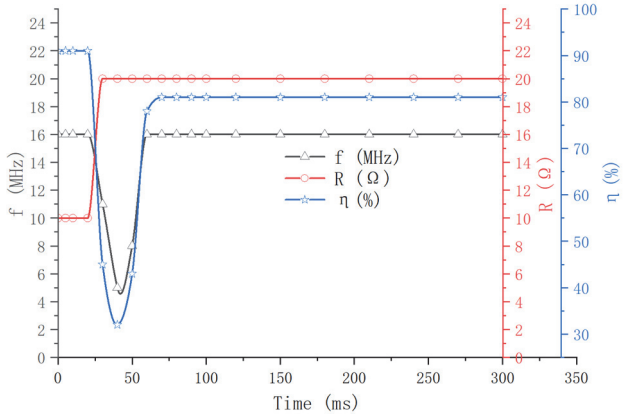

Figure 10 Dynamic tuning performance test under load variation

As can be seen from Fig. 10, the system response time is about 8 ms, the system resonant frequency adjustment time is about 42 ms, the conversion efficiency before the change is 91%, the efficiency after tuning is 81%, and the efficiency recovery accounts for 89%.

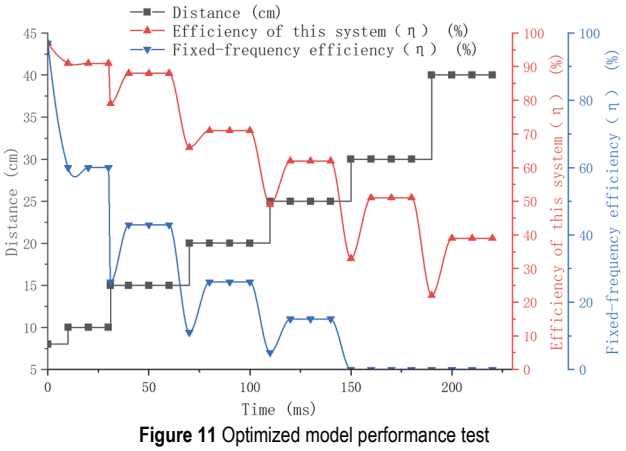

Figure 11 Optimized model performance test

Table 1 Dynamic performance test results

Distance / cm	Fixed-frequency efficiency / %	Efficiency of this system / %	Efficiency improvement / %
10	60.00	91.00	31.00
15	43.00	88.00	45.00
20	26.00	71.00	45.00
25	15.00	62.00	47.00
30	0.04	51.00	50.96
40	0.00	39.00	39.00

In the dynamic distance scenario (8 cm to 40 cm), the transmission efficiency of fixed resonant frequency and the transmission efficiency of the optimized model in this paper are tested, as shown in Tab. 1 and Fig.11.

In Tab. 1 and Fig. 11, the efficiency of the optimized system is improved by 42.99% on average compared with that of the fixed frequency scheme.

6.5 Robustness and Anti-interference Testing

The load is 10 Ω, providing ±30% of the load disturbance and measuring the efficiency change, as shown in Fig.12.

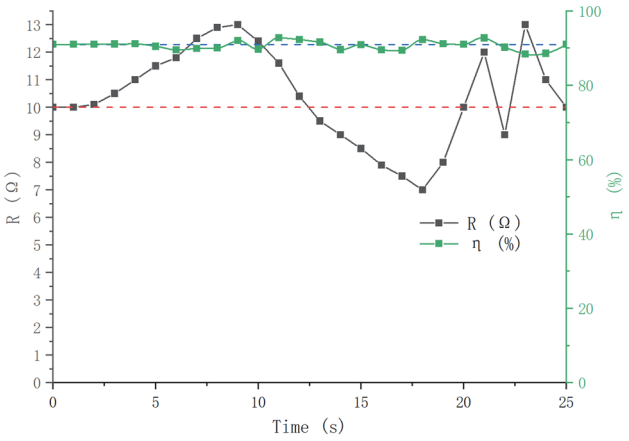

Figure 12 System robustness test

In Fig. 12, when the load varies within the ±30% range, the absolute value of the system transmission efficiency fluctuation reaches a maximum of 1.82%, which is overall less than 2%, indicating that the system has good robustness.

The distance is kept at 10 cm, and a metal obstacle is introduced between the transmitting coil and the receiving coil to test the anti-interference performance of the system. The change of system transmission efficiency is shown in Fig. 13.

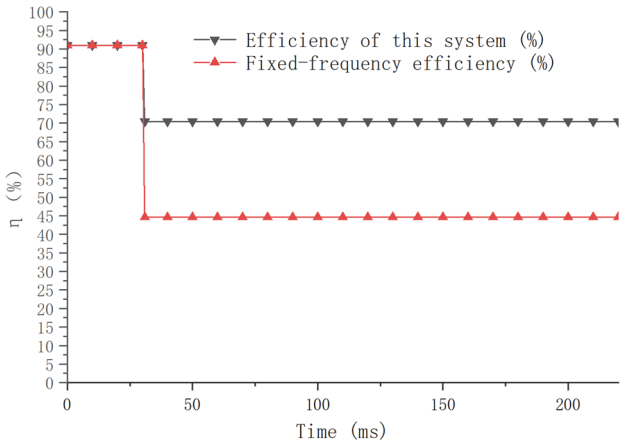

Figure 13 Anti-interference test

As can be seen from Fig. 13, the system maintains an efficiency of 70.4% through dynamic tuning, while the efficiency of the system without the optimization model drops to 44.6%. It shows that the system has good anti-interference performance.

6.6 Comparison of this Algorithm with Traditional Algorithms

The performance of this algorithm is compared with that of LCC compensation, genetic algorithm and differential evolution algorithm. The results are shown in Fig. 14.

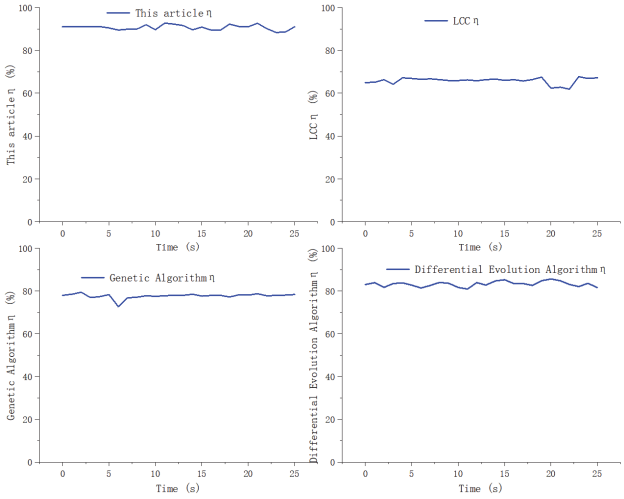

Figure 14 Performance comparison test of different algorithms

In Fig. 14, the efficiency variance of the algorithm in this paper is 1.34; the efficiency variance of the LCC method is 2.84; the efficiency variance of the genetic algorithm is 1.40; and the variance of the differential evolution algorithm is 1.53. The variance of this algorithm is the smallest, indicating that the volatility and dispersion of the data of this method are smaller.

7 CONCLUSION AND FUTURE DIRECTIONS

The adaptive WPT system proposed in this paper significantly improves the energy transmission performance through dynamic tuning and efficiency optimization. Experiments show that the system can maintain high efficiency and stability in complex environments. In actual tests, this method can increase charging efficiency and reduce the risk of overheating. The collaborative tuning of multiple receiving ends can solve the power fluctuation problem when charging multiple vehicles.

During the research, it was found that the circuit's own loss at high frequencies also affects the system's stability. Therefore, further optimization of coil materials and topology structure is needed to reduce loss and improve conversion efficiency.

Future work will focus on the following two points: one is multi-physics field coupling modeling, combined with electromagnetic-thermal coupling analysis, to optimize system safety; the other is AI-driven optimization, introducing deep learning algorithms to achieve more intelligent parameter prediction.

8 REFERENCES

[1] Venkatesan, R., Savio, A. D., Balaji, C., Narayanamoorthi, R., Kotb, H., Elrashidi, A., & Nureldeen, W. (2024). A comprehensive review on efficiency enhancement of wireless charging system for an electric vehicles application. *IEEE Access*. https://doi.org/10.1109/ACCESS.2024.3378303

[2] Tilki, U. & Ölgün, M. (2023). Terminal and back stepping sliding mode control with genetic algorithms for robot manipulators. *Studies in Informatics and Control*, *32*(2), 117-126. https://doi.org/10.24846/v32i2y202311

[3] Behnamfar, M., Olowu, T. O., Tariq, M., & Sarwat, A. (2024). Comprehensive review on power pulsation in dynamic wireless charging of electric vehicles. *IEEE Access*. https://doi.org/10.1109/ACCESS.2024.3397583

[4] Obaideen, K., Albasha, L., Iqbal, U., & Mir, H. (2024). Wireless power transfer: Applications, challenges, barriers, andthe role of AI in achieving sustainable development goals - A bibliometric analysis. *Energy Strategy Reviews*, *53*, 101376. https://doi.org/10.1016/j.esr.2024.101376

[5] Tan, Z., Liu, F., Chan, H. K., & Gao, H. O. (2022). Transportation systems management considering dynamic wireless charging electric vehicles: Review and prospects. *Transportation Research Part E: Logistics and Transportation Review*, *163*, 102761. https://doi.org/10.1016/j.tre.2022.102761

[6] Amjad, M., Farooq-i-Azam, M., Ni, Q., Dong, M., & Ansari, E. A. (2022). Wireless charging systems for electric vehicles. *Renewable and Sustainable Energy Reviews*, *167*, 112730. https://doi.org/10.1016/j.rser.2022.112730

[7] Fayti, M., Mjahed, M., Ayad, H., & Kari, A. E. (2023). Recent meta heuristic-based optimization for system modelling and PID controllers tuning. *Studies in Informatics and Control*, *32*(1), 57-67. https://doi.org/10.24846/v32i1y202306

[8] Ren, X. (2024). Parameter adaptive optimization algorithm of intelligent power system based on Internet of Things technology. *International Journal of Thermofluids*, *21*, 100594. https://doi.org/10.1016/j.ijft.2024.100594

[9] Zhang, M., Zhang, H., Tao, W., Yang, Y., & Sang, Y. (2024). The power control and efficiency optimization strategy of dynamic wireless charging system for multiple electric vehicles. *Circuit World*, *50*(4), 365-379. https://doi.org/10.1108/CW-01-2024-0003

[10] Rajani, D., Gopal, J. V., Saxena, A., Salman, Z. N., & Jain, A. (2024, May). Enhancing electric vehicle charging with dynamic adaptation: A machine learning approach to improving grid alignment precision. *2024 International Conference on Communication, Computer Sciences and Engineering (IC3SE)*, 702-707. https://doi.org/10.1109/IC3SE62002.2024.10593543

[11] Moon, J., Son, M., Oh, B., Jin, J., & Shin, Y. (2024). Automatic voltage stabilization system for substation using deep learning. *Computer Science and Information Systems*, *21*(2), 437-452. https://doi.org/10.2298/CSIS220509050M

[12] Xia, D. X., Han, J. Q., Mu, Y. J., Guan, L., Wang, X., Ma, X. J., ... & Cui, T. J. (2024). Adaptive wireless-powered network based on CNN near-field positioning by a dual-band meta surface. *Nature Communications*, *15*(1), 10358. https://doi.org/10.1038/s41467-024-54800-2

[13] Singh, S. V., Sharma, S., Dutt, A., Monika, S., Mohammed, H., & Deepika, N. M. (2024, May). Revolutionizing dynamic electric vehicle charging: Innovations in inductive power transfer system optimization. *2024 International Conference on Communication, Computer Sciences and Engineering (IC3SE)*, 1270-1275. https://doi.org/10.1109/IC3SE62002.2024.10593066

[14] Rahman, M. S. & Ali, M. H. (2024, March). Development of controllers for compensating misalignment in vehicle-to-vehicle dynamic wireless charging system. *Southeast Con 2024*, 374-379. https://doi.org/10.1109/SoutheastCon52093.2024.10500185

[15] Abideen, S. Z. U., Wahid, A., & Kamal, M. M. (2024). Adaptive security solutions for NOMA networks: The role of DDPG and RIS-equipped UAVs. *International Journal of*

Electrical, Energy and Power System Engineering, *7*(3), 158-174. https://doi.org/10.31258/ijeepse.7.3.158-174

[16] Chu, C. & Ma, H. (2024). Robust compensation with adaptive fuzzy Hermite neural networks in synchronous reluctance motors. *Computer Science and Information Systems, 21*(2), 569-592. https://doi.org/10.2298/CSIS230803076C

[17] Li, W., Wang, Q., Lan, Y. S., & Ma, C. S. (2024). Multi-environment adaptive fast constant false alarm detection algorithm optimization strategy. *Tehnički vjesnik*, *31*(3), 936-944. https://doi.org/10.17559/TV-20230703000781

[18] Rahman, M. S. & Ali, M. H. (2024). Adaptive neurofuzzy inference system (ANFIS) based control for misalignment problem solution to vehicle-to-vehicle dynamic wireless charging system. *Authorea Preprints.* https://doi.org/10.36227/techrxiv.172954514.43347885/v1

[19] Luo, B., Wu, H., Wang, M., Wang, F., Bai, L., Jiang, C., & You, J. (2024). Front-end parameter identification method based on Adam-W optimization algorithm for underwater wireless power transfer system. *IEEE Transactions on Power Electronics.* https://doi.org/10.1109/TPEL.2024.3516493

[20] Yang, L., Yang, B., Yang, G. W., Xiao, S. N., Zhu, T., & Wang, F. (2022). A method for prediction of S-N curve of spot-welded joints based on numerical simulation. *Advances in Production Engineering & Management*, *17*(2), 141-151. https://doi.org/10.14743/apem2022.2.426

[21] TA, A. R. & Marshiana, D. (2025). Adaptive coil and compensation integration design (ACCID) for enhancing wireless charging for electric vehicles with efficient power transfer. *Computers and Electrical Engineering*, *123,* 110184. https://doi.org/10.1016/j.compeleceng.2025.110184

[22] Yue, J., Liu, Z., & Su, H. (2024). Robust voltage regulation in dynamic wireless EV charging systems via dual-frequency oscillation suppression. *IEEE Transactions on Industrial Electronics.* https://doi.org/10.1109/TIE.2024.3503636

[23] Sangeetha, S., Logeshwaran, J., Faheem, M., Kannadasan, R., Sundararaju, S., & Vijayaraja, L. (2024). Smart performance optimization of energy-aware scheduling model for resource sharing in 5G green communication systems. *The Journal of Engineering*, *2024*(2), e12358. https://doi.org/10.1049/tje2.12358

[24] Raska, P., Ulrych, Z., Baloun, J., Malaga, M., & Lenc, L. (2024). Using adaptive neural networks for optimising discrete event simulation. *International Journal of Simulation Modelling*, *23*(2), 227-238. https://doi.org/10.2507/IJSIMM23-2-678

[25] Zhang, M., Liu, Z., & Su, H. (2024). Optimal output regulation for EV dynamic wireless charging system via internal model-based control. *IEEE Transactions on Industrial Electronics*, *71*(10), 13031-13041. https://doi.org/10.1109/TIE.2024.3352158

[26] Sket, K., Ficko, M., Gubeljak, N., & Brezocnik, M. (2023). Study of environmental impacts on overhead transmission lines using genetic algorithms. *International Journal of Simulation Modelling*, *22*(4), 610-618. https://doi.org/10.2507/IJSIMM22-4-661

[27] Yehoshua, A., Bechar, A., Cohen, Y., & Shmuel, L., Edan, Y. (2023). Dynamic sampling algorithm for agriculture-monitoring ground robot. *International Journal of Simulation Modelling*, *22*(3), 392-403. https://doi.org/10.2507/IJSIMM22-3-646

[28] Li, W., Meng, X. Q., & Ma, C. S. (2024). Optimal differential control for accurate positioning of medical electronic wristband. *Tehnički vjesnik*, *31*(3), 792-799. https://doi.org/10.17559/TV-20230809000866

[29] Liu, X., Chao, J., Rong, C., Liao, Z., & Xia, C. (2024). Compatibility and performance improvement of the WPT systems based on Q-learning algorithm. *IEEE Transactions on Power Electronics.* https://doi.org/10.1109/TPEL.2024.3397804

[30] Tang, H., Liu, C., Pan, W., Rao, P., Zhuang, Y., Chen, X., & Zhang, Y. (2024). A self-adaptive dual-channel LCC-S detuned topology for misalignment tolerance in AUV wireless power transfer systems. *IEEE Transactions on Power Electronics.* https://doi.org/10.1109/TPEL.2024.3492194

[31] Liu, X., Jin, D., Ji, H., Liu, L., & Xia, C. (2024). Research on mutual inductance identification and efficiency optimization of the three-coil wireless power transfer systems with switch able relay coil. *IEEE Transactions on Power Electronics*, *39*(5), 6492-6503. https://doi.org/10.1109/TPEL.2024.3363138

[32] Wang, Y., Chen, W., Li, Q., Han, Y., Guo, A., & Wang, T. (2024). Coordinated optimal power distribution strategy based on maximum efficiency range of multi-stack fuel cell system for high-altitude. *International Journal of Hydrogen Energy*, *50*, 374-387. https://doi.org/10.1016/j.ijhydene.2023.08.177

[33] Villalobos, J., Martell, F., & Sanchez, I. Y. (2023). Comparison of model reference control schemes for motor speed control under variable load torque. *Studies in Informatics and Control*, *32*(2), 63-72. https://doi.org/10.24846/v32i2y202306

[34] Li, F. F., Zuo, H. M., Jia, Y. H., & Qiu, J. (2024). A developed Criminisi algorithm based on particle swarm optimization (PSO-CA) for image inpainting. *The Journal of Supercomputing*, *80*(11), 16611-16629. https://doi.org/10.1007/s11227-024-06099-5

Contact information:

Wei LI
(Corresponding author)
School of Electronic Information Engineering,
Geely University of China,
Chengdu, 641423, China
E-mail: li.wei.77@163.com

Qian WANG
School of Electronic Information Engineering,
Geely University of China,
Chengdu, 641423, China

Pei-chun CHEN
International Research Programme Manager,
Research Services, Coventry University,
Coventry, UK